2-2018

Defect-mediated, thermally-activated encapsulation of metals at the surface of graphite

Yinghui Zhou
Ames Laboratory

Ann Lii-Rosales
Iowa State University and Ames Laboratory, ylii@iastate.edu

Minsung Kim
Ames Laboratory, mskim@ameslab.gov

Mark Wallingford
Ames Laboratory

Dapeng Jing
Iowa State University and Ames Laboratory, djing@iastate.edu

See next page for additional authors

Defect-mediated, thermally-activated encapsulation of metals at the surface of graphite

Abstract
We show that 3 metals – Dy, Ru, and Cu – can form multilayer intercalated (encapsulated) islands at the graphite (0001) surface if 2 specific conditions are met: Defects are introduced on the graphite terraces to act as entry portals, and the metal deposition temperature is well above ambient. Focusing on Dy as a prototype, we show that surface encapsulation is much different than bulk intercalation, because the encapsulated metal takes the form of bulk-like rafts of multilayer Dy, rather than the dilute, single-layer structure known for the bulk compound. Carbon-covered metallic rafts even form for relatively unreactive metals (Ru and Cu) which have no known bulk intercalation compound.

Keywords
Graphite, Dysprosium, Ruthenium, Copper, Intercalation

Disciplines
Biological and Chemical Physics | Materials Chemistry | Metallurgy

Comments
This is a manuscript of an article published as Zhou, Yinghui, Ann Lii-Rosales, Minsung Kim, Mark Wallingford, Dapeng Jing, Michael C. Tringides, Cai-Zhuang Wang, and Patricia A. Thiel. "Defect-mediated, thermally-activated encapsulation of metals at the surface of graphite." *Carbon* 127 (2018): 305-311. DOI: 10.1016/j.carbon.2017.10.103. Posted with permission.

Authors
Yinghui Zhou, Ann Lii-Rosales, Minsung Kim, Mark Wallingford, Dapeng Jing, Michael C. Tringides, Cai-Zhuang Wang, and Patricia A. Thiel

Defect-Mediated, Thermally-Activated Encapsulation of Metals at the Surface of Graphite

Yinghui Zhou,[1†‡*] Ann Lii-Rosales,[1,2‡*] Minsung Kim,[1] Mark Wallingford,[1] Dapeng Jing,[1] Michael C. Tringides,[1,3] Cai-Zhuang Wang,[1,3] and P. A. Thiel[1,2,4*]

[1]The Ames Laboratory, Ames, Iowa 50011, USA

[2]Department of Chemistry, Iowa State University, Ames, Iowa 50011, USA

[3]Department of Physics & Astronomy, Iowa State University, Ames, Iowa 50011, USA

[4]Department of Materials Science & Engineering, Iowa State University, Ames, Iowa 50011, USA

KEYWORDS: Graphite, dysprosium, ruthenium, copper, intercalation

ABSTRACT: We show that 3 metals – Dy, Ru, and Cu – can form multilayer intercalated (encapsulated) islands at the graphite(0001) surface if 2 specific conditions are met: Defects are introduced on the graphite terraces to act as entry portals, and the metal deposition temperature is well above ambient. Focusing on Dy as a prototype, we show that surface encapsulation is much different than bulk intercalation, because the encapsulated metal takes the form of bulk-like rafts of multilayer Dy, rather than the dilute, single-layer structure known for the bulk compound. Carbon-covered metallic rafts even form for relatively unreactive metals (Ru and Cu) which have no known bulk intercalation compound.

1. Introduction.

Intercalation in bulk layered materials has long been recognized as a way to alter and tune the transport and magnetic properties of a *bulk* compound over a wide range.[1] However, intercalation at *surfaces* of *bulk* layered compounds has received very little attention, despite the fact that it presents attractive possibilities. For example, intercalation could be an opportunity to tailor transport, catalysis, magnetism, or friction properties at the surface while also protecting the intercalated material. Indeed, this rationale has motivated the scientific community to

* Corresponding author. Email: ylii@iastate.edu (Ann Lii-Rosales)

* Corresponding author. Email: yhzhou@xmu.edu.cn (Yinghui Zhou)

* Corresponding author. Email: thiel@ameslab.gov (Patricia A. Thiel)

examine intercalation beneath supported graphene closely,[2, 3] but it has rarely extended its scope to the surfaces of *bulk* layered materials.

Graphite is a particularly attractive layered material because it is cheap, abundant, and robust. It is the focus of the present work, together with elemental metals as intercalants. Certain elemental metals are known to form bulk graphite intercalation compounds (b-GICs), which consist of single, dilute layers of intercalant separated by one or more graphene sheets. b-GICs are particularly well-known for the alkali metals and alkaline earths, such as Li, Cs, and Ca.[1] For Cs, surface intercalation on graphite has been observed, and the structure is the same as in the b-GIC of Cs.[4] For other types of metals, there are no reports of surface intercalation on graphite to our knowledge, despite numerous investigations of metals deposited on graphite.[5] In this work we investigate one rare earth metal (Dy), and two metals that represent late transition metals (Ru, Cu), with the goal of determining whether experimental conditions can be found that enable surface intercalation. It is thus noteworthy that b-GICs are known for some rare earths, including Dy, but not for transition metals.[6, 7]

We show that two specific conditions are required. First, defects must be introduced on the graphite terraces prior to metal deposition. Second, the metal must be deposited at temperatures well above ambient. This results in multilayer metallic islands that are embedded in the graphite surface, but they are so much different from b-GICs that "encapsulated" may be a better descriptor than "intercalated".

The idea of introducing defects derives from an earlier study of the alkali metal Cs on graphite, where Büttner *et al*.[4] ion bombarded a graphite surface. When Cs was then deposited at room temperature and annealed, Cs formed bulk-like intercalation structures in the surface region. The authors proposed that bombardment-induced defects could serve as portals for surface intercalation of Cs, but only if defects exceeded a certain minimum size related to the number of missing carbon atoms. In the present work, we adopt part of their approach—ion bombardment prior to metal deposition—but their approach of subsequent annealing *to* elevated temperature is ineffective for these metals. Instead, deposition *at* elevated temperature is required. The fact that ion bombardment is part of the process means that it may eventually be possible to pattern the active defects and hence fix the locations of the encapsulated nanostructures.

2. Experimental and Computational Details.

Our experiments were performed in an ultrahigh vacuum (UHV) chamber with base pressure 2×10^{-11} mbar, and equipped with scanning tunneling microscopy (STM). Commercial samples of highly-oriented pyrolytic graphite (HOPG; ZYB grade) were used as substrates for metal deposition. These are expected to have a high degree of perfection along the [0001] direction (perpendicular to the graphene sheets) but to contain micron-size rotational domains within the sheets.[8] The clean pristine surface was prepared by tape-cleavage in air, followed by transfer into UHV and then annealing at 800 K for 20 minutes. The ion-bombarded graphite surface was prepared with subsequent 3 keV Ar^+ bombardment for 30 seconds followed by annealing at 900 K for 2 hours to remove embedded Ar. Details about metal deposition and STM methods are available in the Supplementary Data.

First-principles calculations were based on density functional theory (DFT), as implemented in the VASP package.[9, 10] The projector-augmented wave (PAW) method[11] was used where 4*f* electrons of Dy were kept frozen in the core. Perdew-Burke-Ernzerhof (PBE) exchange-correlation functional was adopted.[12] A plane-wave basis set with energy cutoff 400 eV was used. Dispersion forces were included using the DFT-D3 method.[13] We employed slab geometries, and included sufficient vacuum regions (> 1.8 nm) to prevent unwanted interaction between the periodic slabs.

Two types of configurations were analyzed for Dy: One chosen to mimic the known b-GIC, and a denser configuration to approximate a raft of metallic Dy. The b-GIC-like configuration is a $(\sqrt{3}\times\sqrt{3})R30^{o}$ ($\sqrt{3}$ for short) unit cell of Dy. For this we used 11 AB-stacked graphene layers where the stacking of adjacent layers was set to be AA upon intercalation (consistent with the b-GIC structure), and 15×15×1 *k*-point meshes. For the denser Dy configuration, we used 5 or 7 graphene layers in the slab, depending on the number of Dy layers, and 8×8×1 *k*-point meshes.

3. Experimental Results.

Large-scale STM images (Figure 1a) show that the pristine graphite surface has atomically flat terraces, hundreds of nanometers wide. The atomic order of graphite is resolved at higher magnification (Figure 1b), with the expected atomic spacing of 0.247 ± 0.003 nm (bulk value: 0.246 nm[14]). In contrast, many defects are present after Ar^+ ion bombardment as described in Sec. 2. Figure 1c shows a typical STM image of such a surface, with defect density 0.020 ± 0.003 nm^{-2}. Moreover, the well-known[15] $(\sqrt{3}\times\sqrt{3})R30^\circ$ superstructure can be observed surrounding many defect sites, extending several nanometers from the center of each defect, as shown in Figure 1d.

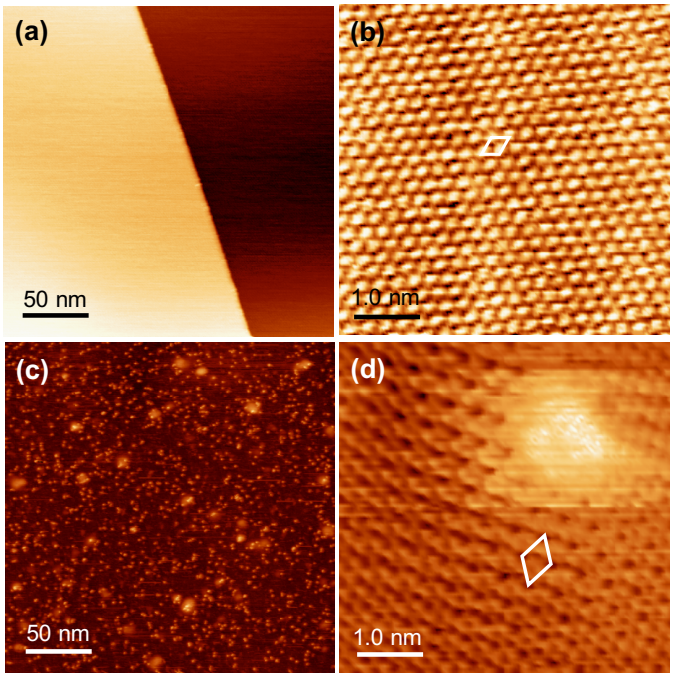

Figure 1. STM images of (a, b) pristine graphite and (c, d) 3 keV Ar^+ bombarded graphite surfaces after heating at 900 K for 2 hours. (b) is a derivative image. The white rhombus in (b) shows the (1×1) unit cell of graphite, while the rhombus in (d) outlines the $(\sqrt{3}\times\sqrt{3})R30^\circ$ supercell surrounding a defect. Tunneling conditions (all tip bias): (a) 0.29 nA, +0.84 V; (b) 0.46 nA, +0.070 V; (c) 0.27 nA, +0.52 V; (d) 0.50 nA, +0.07 V.

Dy was deposited onto these two types of graphite substrates *at* 800-850 K in UHV. On the pristine graphite surface, at this temperature, Dy forms some large faceted islands on the terraces, and heavily decorates the step edges (Figure 2a). In contrast, on the ion bombarded surface, ion-induced defects act as effective trapping sites for Dy and promote the nucleation of Dy clusters on top of graphite terraces (Figure 2b). These Dy clusters show smaller footprints and higher density compared with those on pristine graphite. Besides the surface Dy clusters on

the ion bombarded surface, there exists another type of island with a specific height of 0.61 ± 0.03 nm (n = 54 islands). Examples are encircled in Figure 2b.

If, instead of being deposited *at* 800-850 K, Dy is deposited on the ion bombarded surface at 300 K and then annealed *to* 800 K, the result is much different. Figure 2c shows the result of deposition of Dy on the bombarded surface at 300 K, which produces small Dy clusters. Heating this surface to 800 K causes the small clusters to coarsen, as shown in Figure 2d, but does not produce the 0.6 nm features. They also fail to appear upon heating to this temperature if the graphite surface is initially pristine, as shown by data in the Supplementary Data. Therefore, deposition must be carried out at elevated temperatures on the ion-sputtered surface, to form the special 0.6 nm islands.

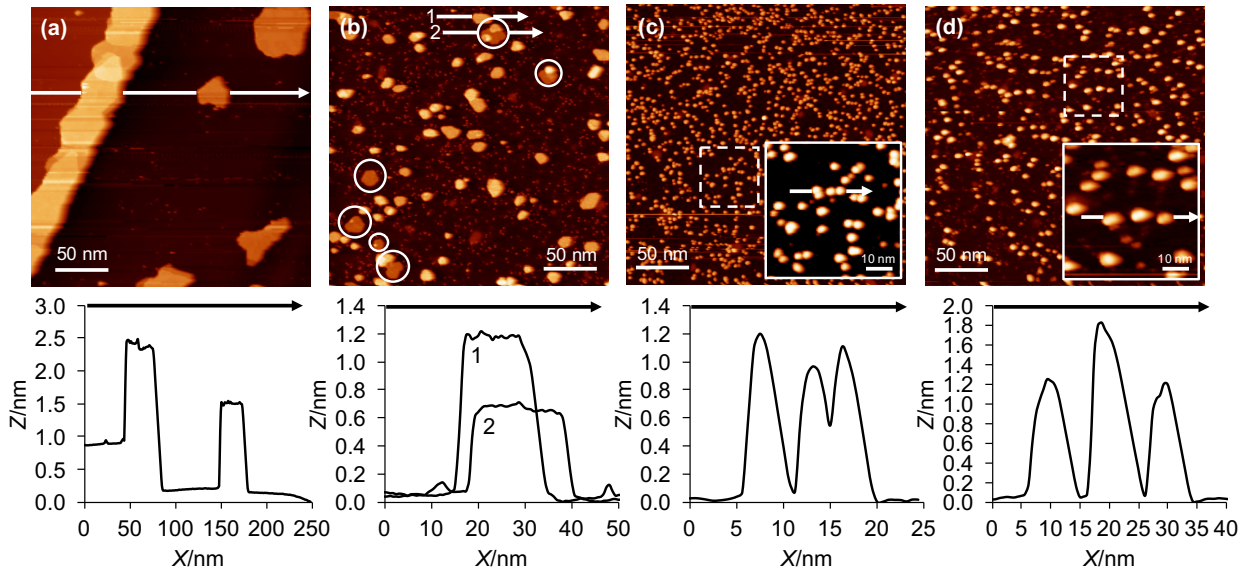

Figure 2. STM images of Dy deposited on: (a) pristine graphite at 800 K; (b) ion bombarded graphite at 800 K; and (c) ion bombarded graphite at 300 K. Panel (d) shows the surface in (c) after annealing to 800 K. In (b), profile #1 crosses a Dy cluster on top of the surface, while profile #2 crosses a 0.6 nm island. Inset in (c) shows enlargement of the area enclosed in the square with dashed lines. Tunneling conditions (all tip bias): (a) 0.18 nA, +1.26 V; (b) 0.26 nA, +0.53 V; (c) 0.25 nA, +1.58 V; (d) 0.25 nA, +2.32 V.

In STM images (Figure 3a, 3b), the 0.6 nm islands are characterized by a flat top, though they often emanate from the base of a taller Dy cluster. The islands often exhibit a faceted shape consistent with hexagonal symmetry, together with a hexagonal moiré pattern having periodicity 1.49 ± 0.10 nm, as shown in Figure 3a', 3b'. The presence of the moiré indicates that the islands are atomically-well-ordered. Islands lacking these two features – moiré and hexagonal shape –

presumably are more disordered. More STM images, produced in different experiments with comparable experimental parameters, are given in the Supplementary Data to demonstrate the robustness of these results.

Superimposed on the moiré is a hexagonal arrangement of features with lateral spacing of 0.247 ± 0.005 nm, which serves to identify this as the atomic graphite lattice. This spacing is distinct from the Dy interatomic spacing in a (0001) plane of bulk Dy, 0.359 nm. The graphite lattice is continuous over the edge of the island, as illustrated in Figure 3(c', c"). The transition region between the substrate and the island is about 1 nm wide.

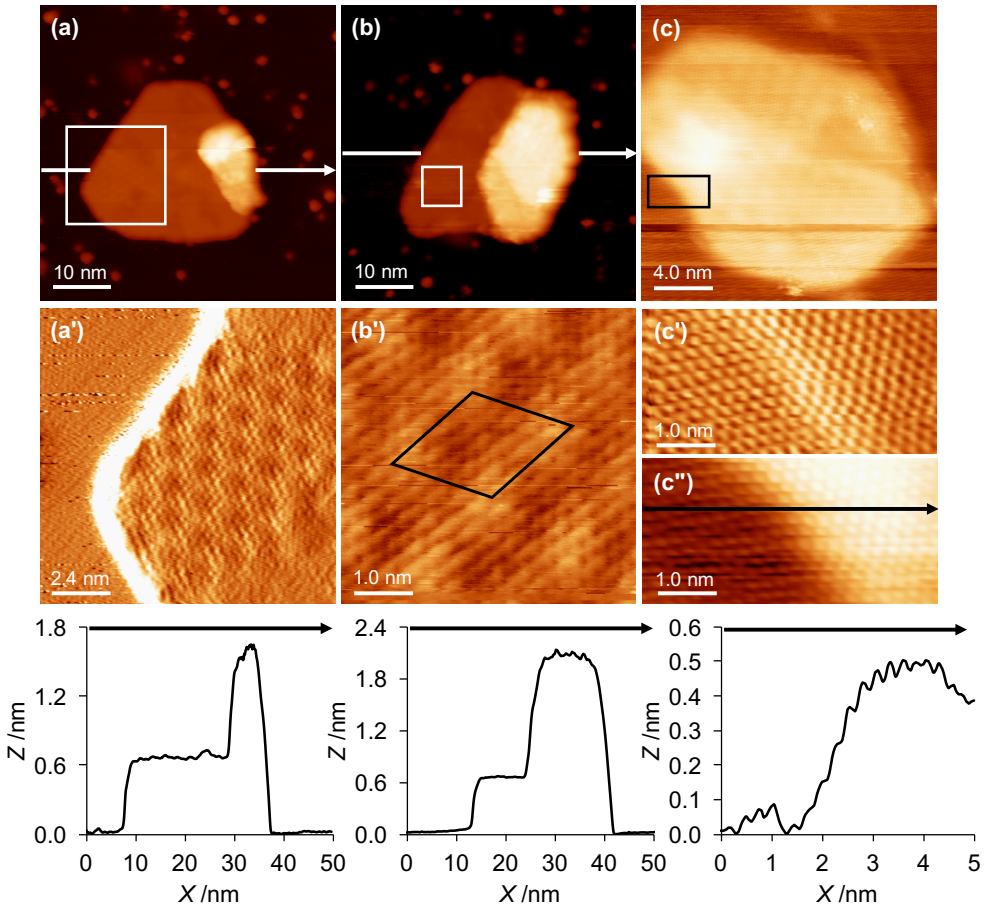

Figure 3. (a, b) STM images of intercalated Dy islands with upper clusters and corresponding profiles. (a', b') Higher-magnification derivative images of regions circumscribed by white rectangles in (a, b), revealing the moiré and graphitic fine structure. Black rhombus in (b') shows the unit cell of the moiré. (c) An intercalated Dy island without any noticeable upper clusters. The graphitic overlayer is continuous around the edge as seen in (c', c"). (c') is a derivative image. The profiles at the bottom correspond to the horizontal arrows in upper panels. Tunneling conditions (all tip bias): (a) 0.25 nA, +1.50 V; (b) 0.25 nA, +1.50 V; (c) 0.28 nA, +0.25 V.

We propose that the 0.6 nm features are islands of Dy, covered by one or more layers of graphene. The moiré is evidence that the Dy is dense (close-packed), which is supported further by the frequent hexagonal footprint. Given that the interplanar spacing between close-packed layers of bulk Dy is 0.283 nm, the measured thickness of 0.6 nm indicates that multiple Dy layers are involved.

To confirm the role of ion bombardment-induced defects in the surface intercalation, we vary the defect density by changing bombardment time and energy. We find that the density of the 0.6 nm islands depends strongly on the defect density, confirming that the defects play an important role. Furthermore, the intercalated island density is consistently a small fraction (~1%) of the corresponding defect density, indicating that only a small fraction of defects is active in promoting intercalation. Following Büttner et al.,[4] we propose that the active defects are entry portals that satisfy a minimum size requirement, hence accounting for the small ratio of 0.6 nm islands to total defects. The requirement of elevated temperature may reflect an activation barrier for passage of metal atoms through the portals, as suggested by Büttner et al.[4] The requirement of *deposition* at elevated temperature, rather than annealing, then indicates that this process can be blocked if Dy islands form at the portals, which occurs at room temperature.

Carbides of Dy are well-known.[16] Elsewhere,[17] we show that a surface carbide can form by reaction between Dy and graphite, but higher temperatures and a different thermal program are required than those used here. The reaction leaves etch pits in the graphite surrounding to the islands, reflecting consumption of carbon. The carbide islands themselves exhibit a distinctive appearance. Their tops are rough and striated, with no evidence of the carbon honeycomb lattice that characterizes the intercalated Dy islands. Etch pits or striated tops are never observed for the 0.6 nm islands, indicating that the intercalated islands of Figure 3 are not carbide.

We have explored whether other metals exhibit surface intercalation on ion-damaged graphite. Figure 4 shows representative results for Ru and Cu. Islands are visible, covered by a well-resolved lattice of graphitic carbon that is continuous from the graphite substrate to the top of the metal island. The minimum deposition temperature required for encapsulation is 900 K and 600 K, respectively. In the case of Ru, the island heights fall in a narrow range of 0.6-1.0 nm. For Cu, heights are larger and more diverse, up to 30 nm. The details of surface intercalation are thus metal-specific, but the general phenomenon occurs in multiple systems. Notably,

neither Ru nor Cu forms a b-GIC. Further STM data are shown in the Supplementary Data for Cu and Ru.

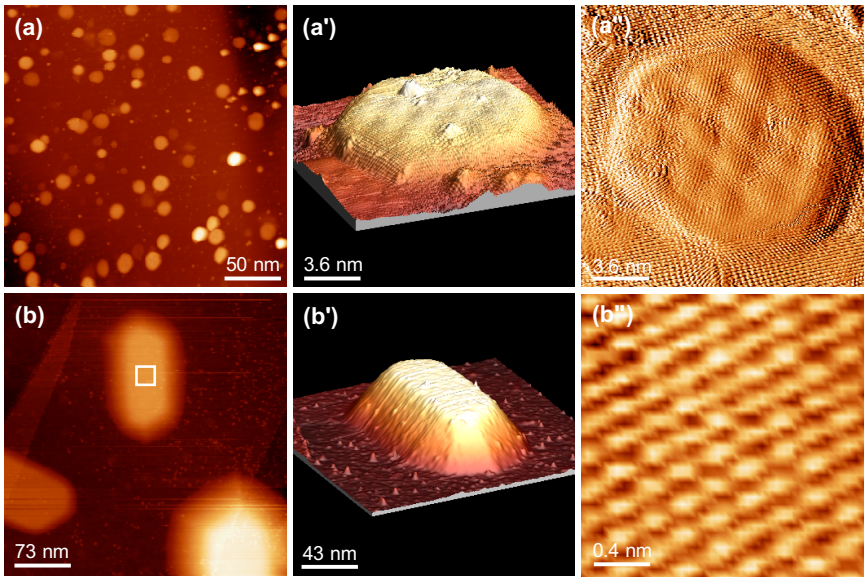

Figure 4. (a) A large-scale STM image showing surface intercalated Ru islands on a terrace. (a', a") 3D image of a Ru island and a derivative image showing moiré patterns atop the island. The entire image of (a") is atomically resolved, i.e. the graphite lattice is seen on the substrate, island edges, and island top. (b) A large-scale STM image of encapsulated Cu islands. (b') is a 3D image of the middle island in (b). (b") shows the atomically-resolved graphite lattice on top of island in (b) as denoted by a white square. Tunneling conditions (all voltages are tip bias) are: (a) 0.26 nA, +1.80 V; (a', a") 0.41 nA, +5 mV; (b, b') 0.26 nA, +4.26V; (b") 0.41 nA, +27.7 mV.

4. Computational Results and Energetic Considerations.

For Dy, we have carried out detailed calculations that provide insight into two types of configurations, represented in the inset to Figure 5. The first type of configuration is an intercalated structure with a $(\sqrt{3}\times\sqrt{3})R30^{o}$ ($\sqrt{3}$ for short) unit cell that mimics the known GIC of Dy.[7] We analyze this for variable numbers (n) of Dy layers, with each pair separated by a graphene sheet. We also analyze its adsorbed (non-intercalated) counterpart for a single Dy layer. Values $n > 1$ for this configuration are not physically realistic.

The second type of configuration is based on a denser layer of Dy, chosen to mimic a close-packed plane of bulk Dy. A c(3×3) unit cell is selected because it provides a reasonable match between the bulk lattice constants of Dy and graphite, while remaining computationally tractable. The c(3×3) has in-plane tensile strain of 2.8% and corresponding reduction in layer

density of 5.4%, relative to bulk Dy. The experimental moiré pattern shows that the coincidence lattice is larger than c(3×3), so this is only an approximation to the real system. We analyze this denser intercalated configuration also for various n, but here the Dy layers were vertically contiguous, comprising a raft of bulk-like intercalated Dy. We also evaluate its adsorbed (bare) counterpart for the same range of n.

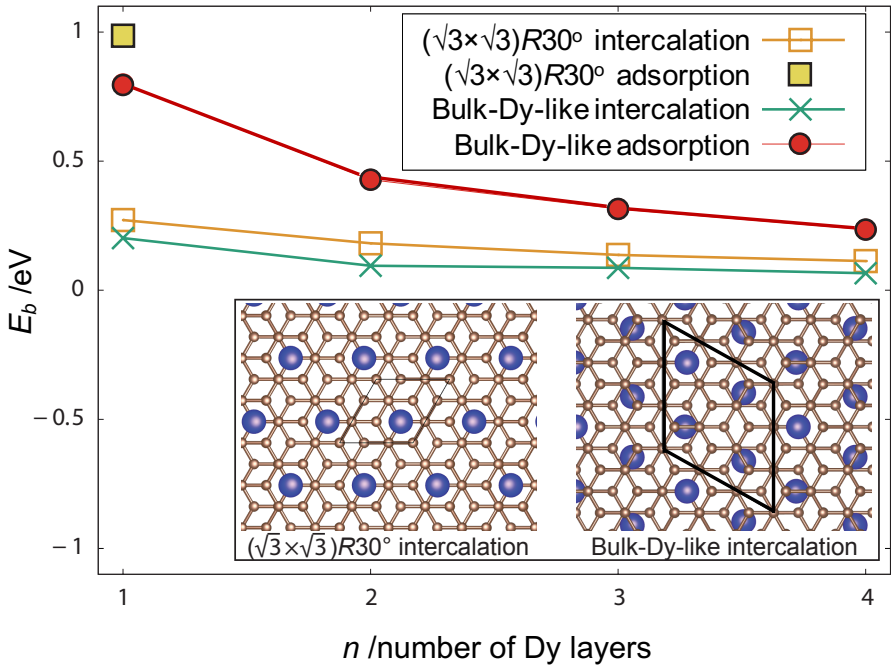

Figure 5. Average binding energy per Dy atom, for GIC-like and bulk-like Dy islands, from DFT. The insets at bottom are views of the models for two types of intercalated, single-layer Dy islands. In each case, the view is perpendicular to the graphite basal plane. The black rhombus shows the c(3×3) unit cell.

To assess relative stabilities, we define the average binding energy of Dy in each configuration as:

$$E_b = (E_{grph+Dy} - E_{grph} - N_{Dy} \times E_{bulk,Dy})/N_{Dy} \qquad (1)$$

where E_{grph}, $E_{bulk,Dy}$, and $E_{grph+Dy}$ denote the energies of graphite, bulk Dy (per atom), and the total system (i.e., graphite with Dy intercalation or adsorption), respectively, and N_{Dy} is the number of Dy atoms.

Results are shown in Figure 5 for $1 \le n \le 4$. The two lower curves show E_b for both intercalated configurations, while the upper curve shows E_b for the adsorbed bulk-like configuration, and a single point at $n = 1$ shows E_b for the adsorbed $\sqrt{3}$ configuration. The adsorption (on-top) configurations are always less stable (E_b more positive) than the intercalated configurations at given n, consistent with the observation of intercalation. For the bulk-like configuration, the energy difference drops from 0.71 eV at $n = 1$, to 0.17 eV at $n = 4$. However, at all n investigated, there is a net driving force for adsorbed Dy to transform into intercalated layers.

Furthermore, the two lower curves show that for a given n, $\sqrt{3}$ intercalation is always less stable than bulk-like intercalation. This is consistent with the fact that in experiments, there is no evidence for surface $\sqrt{3}$ intercalation.

The optimized models also provide vertical island heights h, which can be compared with experiment. Here h is defined as the separation between the two carbon sheets immediately adjacent to the raft on top and bottom, as shown in Figure 6. For comparison with the measured height w of 0.61 ± 0.03 nm, h must be corrected by the spacing between carbon sheets without intercalation, which is 0.34 nm.[14] For the bulk-like intercalation model, the best match is at $n = 3$, where $h = 1.03$ nm, corresponding to $w = 0.69$ nm. Adding or subtracting Dy layers changes w by about 0.28 nm per layer. For the $\sqrt{3}$ GIC-like intercalation model, the best match is at $n = 5$, where $w = 0.65$ nm. Since both experiment and theory provide support for the bulk-like model, we conclude that the intercalated Dy islands are 3-layer bulk-like rafts.

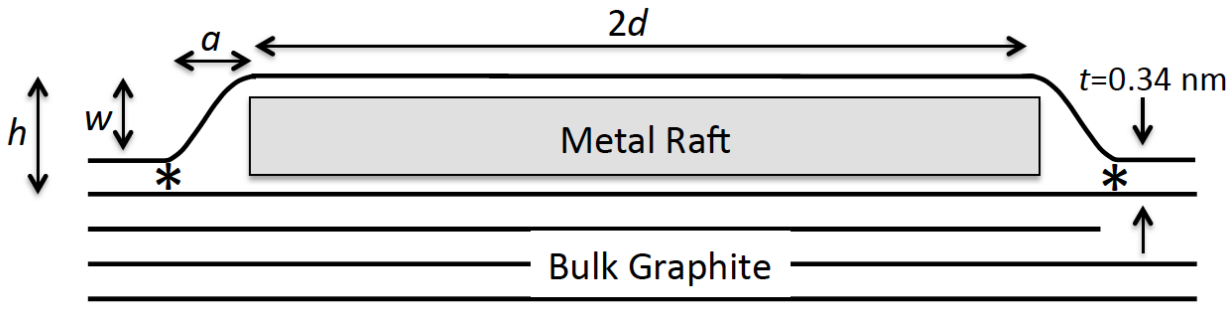

Figure 6. Schematic of encapsulated raft. The asterisks denote points where the top graphene sheet is assumed pinned, for purposes of calculating the work of distortion (see text).

Another perspective on the energetics is provided by considering the energy changes associated with removing a layer of graphene from a graphite surface, and placing it on top of a bare Dy island. In this hypothetical process, a graphite-graphene interface is lost, and a Dy-graphene interface is created. The respective energy changes correspond to the work of adhesion between graphene and graphite, W_{GnGt}, and the negative of the work of adhesion between Dy and graphene, $-W_{DyGn}$. A recent report gives $W_{GnGt} = 0.22 \pm 0.01$ Jm^{-2}.[18] From DFT, we calculate $W_{DyGn} = 1.25$ Jm^{-2}, for 3 layers of adsorbed, bulk-like Dy with the c(3×3) structure shown in Figure 5. The result is that the net energy change for encapsulation is -1.0 Jm^{-2}, where the negative sign indicates that the process is energetically favored. Notably, W_{DyGn} rests on the c(3×3) approximation for the bulk-Dy-like overlayer structure. The real structure is probably more dense, like the bulk metal, which would likely lead to larger magnitudes of W_{DyGn} and the energy of encapsulation, because of the increased metal-graphite contact per unit area.

We now turn attention to the work of distorting the graphene layer around the metal island, W_d. An applicable model was developed by Wan[19] to describe the contact mechanics of a flat punch adhered to a flexible membrane with a fixed circumference. The geometry of the flexible membrane is the same as that of the top graphene layer in Figure 6. To match the constraints of the model, we assume that the graphene sheet is pinned at the lower edges of the islands (marked by * in Figure 6). Furthermore, the model assumes linear elasticity in the film. For a typical Dy island, the strain, based on the increase in length of the top graphene sheet between pinning sites, is 1.5%. This is indeed within the linear elastic regime for graphene.[20, 21]

Then from Eq. (4) of Ref. [19],

$$W_d = \frac{\pi Y t w^4}{(d+a)^2\left(1-\nu^2\right)\left(1-\varsigma^2\right)ln^2\left(\varsigma^2\right)} \qquad (2)$$

In this equation, three parameters are specific to the graphene membrane: Young's modulus (Y) ~ 1 TPa,[20, 21]; Poisson's ratio (ν) ~ 0.17,[20, 21]; and sheet thickness (t) ~ 0.34 nm for a single graphene layer. Other parameters refer to island dimensions, for which typical parameters are: top radius (d) ~ 10 nm; edge width (a) ~ 1 nm (cf. Fig. 3c'); height (w) = 0.61 nm; and

$\zeta = d/(d+a) \sim 0.83$. This results in $W_d = 1.8 \times 10^{-16}$ J for a single island or, normalized to island area, $W_d = 0.6$ Jm^{-2}.

Thus, the energy cost of straining and distorting the graphene film for a typical island geometry, 0.6 Jm^{-2}, is comparable to the energy gained by creating the Dy-graphene interface, 1.0 Jm^{-2}. Since W_d depends very strongly on the height of the island, w, it is possible that strain in the graphene film limits island height in this system.

5. Conclusions.

We have shown that several metals – Dy, Ru, and Cu – can be encapsulated at the graphite(0001) surface. The evidence for encapsulation (intercalation) is the carbon honeycomb lattice on top of the islands, which drapes continuously over the island edges to the graphite support. We focus on Dy as a prototype. The existence of a long-range moiré on the island, and the hexagonal footprint, both indicate that the encapsulated Dy takes the form of atomically-ordered, hexagonally-close-packed layers. DFT confirms that intercalated configurations are more stable than adsorbed (bare) configurations. DFT also shows that surface intercalation in the form of bulk-like slabs is slightly favored over b-GIC-like intercalation, consistent with experimental observations. Estimates of energetic quantities indicate that the energy cost of deforming the carbon sheet is comparable to the energy gain associated with creating a Dy-graphene interface.

We emphasize that these bulk-like multilayer intercalated or encapsulated metal islands are distinct from features observed in three other related systems: b-GICs; metals intercalated between a graphene sheet and a non-graphitic support; and Cs intercalation on ion-bombarded HOPG.[4] In all these three cases, a non-bulk-like, more dilute, single layer of metal forms between graphene sheets (or between graphene and the support).

From the experimental data, intercalation requires pre-existing defects on the graphite surface, and the intercalated island density scales with defect density. Intercalation also requires elevated deposition temperature, suggesting an activated process such as passage of individual metal atoms through the portal. This synthesis strategy is distinct from that used in the study of Cs intercalation on HOPG.[4] For that system, intercalation was achieved by post-deposition annealing (which is not effective for the metals which we have considered), as opposed to deposition at elevated temperatures.

Present Addresses

† Collaborative Innovation Center for Optoelectronic Semiconductors and Efficient Devices, Department of Physics, Xiamen University, Xiamen 361005, China.

Author Contributions

The manuscript was written through contributions of all authors. All authors have given approval to the final version of the manuscript. ‡These authors contributed equally.

Supplementary Data

Additional experimental details, STM images of intercalated metal islands, and assessment of the energetics of encapsulated metal islands are available in the Supplementary Data.

Acknowledgement

This work was supported by the US Department of Energy (DOE), Office of Science, Basic Energy Sciences, Materials Sciences and Engineering Division. Research was performed at the Ames Laboratory, which is operated by Iowa State University under contract # DE-AC02-07CH11358. DFT was performed, in part, with a grant of computer time at the National Energy Research Scientific Computing Centre (NERSC). NERSC is a DOE Office of Science User Facility supported by the Office of Science of the U.S. Department of Energy under Contract No. DE-AC02-05CH11231. YZ's participation in the experimental effort was supported by the China Scholarship Council. We thank J. W. Evans, Scott Bunch, Barbara Lograsso, and Rong Long for enlightening discussions. We thank Emma Kwolek for providing some of the data shown in the Supplementary Data.

References

[1] M.S. Dresselhaus, G. Dresselhaus, Intercalation Compounds of Graphite, Adv. Phys., 51 (2002) 1-186.
[2] M. Batzill, The surface science of graphene: Metal interfaces, CVD synthesis, nanoribbons, chemical modifications, and defects, Surf. Sci. Rep., 67 (2012) 83-115.
[3] X. Liu, Y. Han, J.W. Evans, A.K. Engstfeld, R.J. Behm, M.C. Tringides, M. Hupalo, H.-Q. Lin, L. Huang, K.-M. Ho, D. Appy, P.A. Thiel, C.-Z. Wang, Growth morphology and properties of metals on graphene, Progr. Surf. Sci., 90 (2015) 397-443.
[4] M. Büttner, P. Choudhury, J. Karl Johnson, J.T. Yates Jr., Vacancy clusters as entry ports for cesium intercalation in graphite, Carbon, 49 (2011) 3937-3952.
[5] D. Appy, H. Lei, C.-Z. Wang, M.C. Tringides, D.-J. Liu, J.W. Evans, P.A. Thiel, Transition Metals on the (0001) Surface of Graphite: Fundamental Aspects of Adsorption, Diffusion, and Morphology, Prog. Surf. Sci., 89 (2014) 219-238.
[6] E. Toshiaki, S. Masatsugu, E. Morinobu, Graphite Intercalation Compounds and Applications, Oxford University Press, New York, 2003.

[7] R. Hagiwara, M. Ito, Y. Ito, Graphite intercalation compounds of lanthanide metals prepared in molten chlorides, Carbon, 34 (1996) 1591-1593.
[8] N. Ferralis, K. Pussi, S.E. Finberg, J. Smerdon, M. Lindroos, R. McGrath, R.D. Diehl, Low-energy electron diffraction study of potassium adsorbed on single-crystal graphite and highly oriented pyrolytic graphite, Phys. Rev. B, 70 (2004) 245407.
[9] G. Kresse, J. Hafner, Ab initio molecular dynamics for liquid metals, Phys. Rev. B, 47 (1993) 558-561.
[10] G. Kresse, J. Furthmüller, Efficient iterative schemes for ab initio total-energy calculations using a plane-wave basis set, Phys. Rev. B, 54 (1996) 11169-11186.
[11] P.E. Blöchl, Projector augmented-wave method, Phys. Rev. B, 50 (1994) 17953-17979.
[12] J.P. Perdew, K. Burke, M. Ernzerhof, Generalized Gradient Approximation Made Simple, Phys. Rev. Lett., 77 (1996) 3865-3868.
[13] S. Grimme, J. Antony, S. Ehrlich, H. Krieg, J. Chem. Phys., 132 (2010) 154104.
[14] D.D.L. Chung, Review Graphite, J. Mater. Sci., 37 (2002) 1475-1489.
[15] H.A. Mizes, J.S. Foster, Long-range electronic perturbations caused by defects using scanning tunneling microscopy, Science, 244 (1989) 559-562.
[16] F.H. Spedding, K. Gschneidner Jr, A.H. Daane, J. Am. Chem. Soc., 80 (1958) 4499.
[17] A. Lii-Rosales, Y. Zhou, M. Wallingford, C.-Z. Wang, M.C. Tringides, P.A. Thiel, Formation of dysprosium carbide on the graphite (0001) surface, Phys. Rev. Mater., 1 (2017) 026002.
[18] J. Wang, D.C. Sorescu, S. Jeon, A. Belianinov, S.V. Kalinin, A.P. Baddorf, P. Maksymovych, Atomic intercalation to measure adhesion of graphene on graphite, Nat. Commun., 7 (2016).
[19] K.-T. Wan, Adherence of an axisymmetric flat punch on a thin flexible membrane, J. Adhesion, 75 (2001) 369-380.
[20] G.X. Cao, Atomistic Studies of Mechanical Properties of Graphene, Polymers, 6 (2014) 2404-2432.
[21] C. Lee, X. Wei, J.W. Kysar, J. Hone, Measurement of the elastic properties and intrinsic strength of monolayer graphene, Science, 321 (2008) 385-388.